Archives of Biochemistry and Biophysics 636 (2017) 1–10

Contents lists available at ScienceDirect

Archives of Biochemistry and Biophysics

journal homepage: www.elsevier.com/locate/yabbi

Naringin prevents the inhibition of intestinal Ca^{2+} absorption induced by a fructose rich diet

V. Rodríguez[1], M. Rivoira[1], S. Guizzardi, N. Tolosa de Talamoni*

Laboratorio "Dr. Cañas", Cátedra de Bioquímica y Biología Molecular, Facultad de Ciencias Médicas, INICSA (CONICET-Universidad Nacional de Córdoba), Córdoba, Argentina

ARTICLE INFO

Keywords:
Fructose rich diet
Naringin
Intestinal Ca^{2+} absorption
Oxidative stress
Inflammation
Nitrosative stress

ABSTRACT

This study tries to elucidate the mechanisms by which fructose rich diets (FRD) inhibit the rat intestinal Ca^{2+} absorption, and determine if any or all underlying alterations are prevented by naringin (NAR). Male rats were divided into: 1) controls, 2) treated with FRD, 3) treated with FRD and NAR. The intestinal Ca^{2+} absorption and proteins of the transcellular and paracellular Ca^{2+} pathways were measured. Oxidative/nitrosative stress and inflammation parameters were evaluated. FRD rats showed inhibition of the intestinal Ca^{2+} absorption and decrease in the protein expression of molecules of both Ca^{2+} pathways, which were blocked by NAR. FRD rats showed an increase in the superoxide anion, a decrease in the glutathione and in the enzymatic activities of the antioxidant system, as well as an increase in the NO content and in the nitrotyrosine content of proteins. They also exhibited an increase in both IL-6 and nuclear NF-κB. All these changes were prevented by NAR. In conclusion, FRD inhibit both pathways of the intestinal Ca^{2+} absorption due to the oxidative/nitrosative stress and inflammation. Since NAR prevents the oxidative/nitrosative stress and inflammation, it might be a drug to avoid alteration in the intestinal Ca^{2+} absorption caused by FRD.

1. Introduction

The intestinal Ca^{2+} absorption is an active process that mainly occurs in the small intestine [1]. To obtain an optimal Ca^{2+} absorption, it is necessary to maintain the proper intestinal redox state [2]. The depletion in the intestinal glutathione (GSH) content is associated with a reduction in the Ca^{2+} transport [3], as a consequence of developing oxidative stress, which leads to apoptosis of epithelial cells [4]. Ca^{2+}enters the organism crossing the enterocytes (transcellular pathway) or the intercellular spaces (paracellular pathway). The transcellular pathway involves Ca^{2+} entry through the brush border membranes (BBM or apical border), a process in which the epithelial Ca^{2+} channels such as TRPV6 and TRPV5 participate; movement from one pole to the other of the cells, which is facilitated by the calbindin D_{9k} (CB D_{9K}) and the exit across the basolateral membranes (BLM), where the plasma membrane Ca^{2+}-ATPase and the Na^{+}/Ca^{2+} exchanger are located to pump Ca^{2+} out against the electrochemical gradient [5,6]. The paracellular Ca^{2+} movement occurs through the tight junctions, and presumably involves proteins such as Cldn-2 and Cldn-12 [7].

There is considerable evidence that fructose rich diet (FRD) causes adverse metabolic perturbations. Many studies have demonstrated that FRD to normal rats induces several features of the metabolic syndrome [8,9]. In addition, it has been found that FRD inhibits intestinal Ca^{2+} absorption and induces vitamin D insufficiency [10,11]. The authors claim that the inhibitory effect of fructose on intestinal Ca^{2+} absorption is specific because the sugar has no affect the transepithelial Pi transport and transapical glucose uptake. The underlying mechanisms of the inhibitory effect of fructose on the intestinal Ca^{2+} absorption are not completely elucidated.

Since FRD is known to cause oxidative stress and inflammation in different tissues [12–14], it is quite possible that the inhibitory effect of FRD on intestinal Ca^{2+} absorption involves exacerbation of ROS and inflammatory cytokines, which could alter the functioning of molecules that participate in the intestinal Ca^{2+} transport. If so, the use of antioxidants could block or avoid, at least in part, the inhibitory action of FRD on intestinal Ca^{2+} transport. Flavonoids are considered very potent natural antioxidants. They are polyphenolic compounds ubiquitously found in plants with positive effects against diverse pathologies such as cancer, neurodegenerative or cardiovascular disease [15]. Among them, naringin (full name, naringenin-7-O-neohesperidin glycoside, NAR) is a flavanone that facilitates the removal of free radicals,

* Corresponding author. Cátedra de Bioquímica y Biología Molecular, Facultad de Ciencias Médicas, Universidad Nacional de Córdoba, Pabellón Argentina, 2do. Piso, Ciudad Universitaria, 5000 Córdoba, Argentina.
E-mail addresses: ntolosatalamoni@yahoo.com.ar, ntolosa@biomed.fcm.unc.edu.ar (N. Tolosa de Talamoni).
[1] Have equally contributed.

http://dx.doi.org/10.1016/j.abb.2017.11.002
Received 25 September 2017; Received in revised form 1 November 2017; Accepted 4 November 2017
Available online 07 November 2017
0003-9861/

Abbreviations

AP	alkaline phosphatase
BMI	body mass index
CAT	catalase
CB D_{9K}	calbindin D_{9k}
CLDN 2	claudin 2
CLDN 12	claudin 12
DAB	3,3′-diaminobenzidine
ECLIA	electro-chemiluminescence
FRD	fructose rich diet
GSH	glutathione
HOMA-IR	homeostasis model assessment
IL-6	interleukin 6
NAR	naringin
NBT	nitro blue tetrazolium
$NO^{\bullet}$	nitric oxide
$^{\bullet}O_2^-$	superoxide anion
$PMCA_{1b}$	Ca^{2+}-ATPase
RIA	radioimmunoassay
RIPA	radio immuno precipitation assay buffer
SOD	superoxide dismutase
TG	triglycerides
TRPV6	transient receptor potential cation channel V6
VDR	vitamin D receptor

oxidative stress and inflammation [16]. It is widely distributed in grapefruit and other citrus as well as in Chinese herbal medicines such as *Drynaria fortunei* [17], and it has interesting biological and pharmacological actions due to its antioxidant, antiapoptotic and anti-inflammatory properties [18].

Based upon previous considerations, the aim of this work was to clarify the mechanisms by which FRD causes inhibition of intestinal Ca^{2+} absorption in experimental animals, and determine if any or all underlying alterations are prevented by NAR administration.

2. Material and methods

2.1. Chemicals

All reagents were purchased from Sigma-Aldrich (St. Louis, MO, USA), unless otherwise stated.

2.2. Animals and experimental design

After weaning, male Wistar rats (150–200 g) were fed a commercial normal rodent diet (GEPSA mouse-rat, Pilar, Buenos Aires, Argentina) under standard conditions of humidity, temperature (20-25 °C) and light (12 h light/12 h dark). They had access to water and food *ad libitum* (control group). At two-months old, the animals were divided into three groups: a) controls, b) FRD: the same diet plus 10% fructose (Anedra, Research AG S.A., Buenos Aires, Argentina) in the drinking water during 30 days, c) FRD + NAR40: three days after fructose treatment, a group of rats received daily NAR (40 mg/kg b.w.) therapy *via* subcutaneous injection (Fig. 1). After 30 days of treatment and an overnight fast, they were weighed and killed by cervical dislocation. The excised duodena were rinsed with cold 0.15 M NaCl and mucosa or enterocytes were isolated, as described below. In some experiments other NAR doses were utilized (see Results).

The studies were conducted according to the Guide for Care and Use of Laboratory Animals. The protocol was approved by the CICUAL (Res. 07/15, Commission for Care and Use of Laboratory Animals, Facultad de Ciencias Médicas, Universidad Nacional de Córdoba, Córdoba, Argentina. All efforts were made to minimize the number of animals used and their suffering.

2.3. Serum measurements

Blood samples from rats were used for serum biochemical determinations. Serum glucose (Glicemia enzimática AA), triglycerides (TG Color, GPO/PAP AA), cholesterol (Colestat enzimático AA), HDL (HDL Cholesterol- Precipitating Reagent), LDL (LDL-Cholesterol, monophase AA), Ca (Ca-Color AA), P (Fosfatemia UV-AA) were determined using kits from Wiener Laboratorios S.A.I.C. (Rosario, Argentina) following the manufacturer's protocol. Serum insulin was measured by radioimmunoassay (RIA) using an anti-rat insulin antibody (Sigma, St. Louis, Missouri, USA); the minimum detectable concentration was 0.04 ng/mL 25(OH)D_3 (Vitamin D total, Roche Diagnostics) was measured by electro-chemiluminescence (ECLIA) immunoassay (Modular Analytics E1701, Roche, Mannheim, Germany) and IL-6 by ELISA (Mouse IL-6 ELISA Set, BD OptEIA, San Diego, CA, USA) according to manufacturer's operating protocol.

The insulin resistance was evaluated by the homeostasis model assessment (HOMA-IR) as follows: HOMA-IR = serum insulin (μIU/mL) × fasting blood glucose (mM)/22.5 [19].

2.4. Intestinal calcium absorption

Animals from different groups were anesthetized with an intramuscular injection of ketamine (50 mg/kg b.w.) and xylazine (10 mg/kg b.w), were laparotomized and a 10 cm segment of duodenum was ligated. One milliliter of 150 mM NaCl, 1 mM $CaCl_2$, plus 1.85×10^5 Bq $^{45}Ca^{2+}$, pH 7.2, was introduced into the lumen of the ligated intestinal segment. After 10 min, blood was withdrawn by cardiac puncture, centrifuged and the plasma $^{45}Ca^{2+}$ was measured in a liquid scintillation counter. Absorption was defined as appearance of $^{45}Ca^{2+}$ in blood [2].

2.5. Duodenal cell isolation

Duodenum epithelial cells were isolated as previously described [21]. Villus tip cells were collected by centrifugation at 500×*g* for 5 min, and then resuspended in an incubation medium (140 mM NaCl, 5 mM KCl, 20 mM HEPES, 1 mM $MgCl_2$, 1 mM $CaCl_2$ and 10 mM glucose, pH 7.4). Alkaline phosphatase (AP, EC 3.1.3.1.) activity was performed as a marker enzyme of cell maturation [20]. Cell viability was assessed by the Trypan blue exclusion technique. Only mature cells were used for the different experiments.

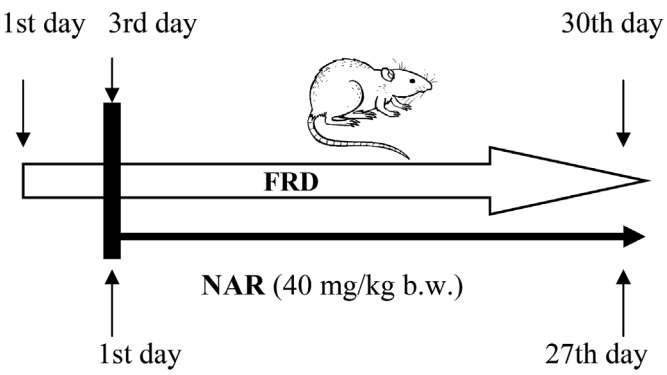

Fig. 1. Schematic diagram of treatment protocol. FRD: fructose-rich diet; NAR: naringin.

2.6. Calcium uptake

The intestinal Ca^{2+} uptake by enterocytes was accomplished by using the technique of Liang et al. [21], with slight variations. An aliquot of 300 μL of cell suspension with 5 g of protein/L was incubated with an uptake solution (140 mM KCl, 10 mM HEPES, 2 mM $CaCl_2$ pH 7.4 *plus* 1.85 × 10^8 Bq/L of $^{45}CaCl_2$). After 10 min, the Ca^{2+} uptake was stopped with 1 mL of the same solution free of ^{45}Ca *plus* 2 mM EGTA, and the mixture was centrifuged 1 min at 10,000 × *g*, which was repeated twice. The final pellet was resuspended in 1 M NaOH solution. Radioactivity was measured in a liquid scintillation counter Beckman LS 6500 (Fullerton, Ca, USA).

2.7. AP activity assay

AP activity was performed by following an adaptation of Walter and Schütt´s method [3]. AP was determined in water homogenates (1:10) of intestinal mucosa using *p*-nitrophenyl phosphate as substrate in 0.5 M diethanolamine buffer pH 9.8. Enzyme activities are expressed in IU/mg of protein.

2.8. Total GSH determination

Total GSH content was measured spectrophotometrically in supernatants from intestinal homogenates using the glutathione disulfide reductase-5,5′-dithiobis (2-nitrobenzoate) recycling procedure, as described elsewhere [22]. The data are expressed in nmol/mg of protein.

2.9. Superoxide anion and protein carbonyl content measurements

Mature duodenal cells were washed twice with Hanks buffer (137 mM NaCl, 5.4 mM KCl, 0.25 mM Na_2HPO_4, 0.44 mM KH_2PO_4, 1.3 mM $CaCl_2$, 1 mM $MgSO_4$, 4.2 mM $NaHCO_3$, 6.24 mM glucose, pH 7.4) and incubated with nitro blue tetrazolium (NBT) (1 mg/mL) at 37 °C for 1 h. The formazan precipitates formed were dissolved in dimethylsulfoxide and quantified by spectrophotometry at 560 nm. OD values are direct indicators of superoxide anion ($O_2^{\cdot -}$) concentration in the samples [23]. The protein carbonyl content was determined by using 2,4-dinitrophenylhydrazine in an aliquot from homogenates of scraped duodenal mucosa diluted in an isolation buffer (50.3 mM HEPES, 127 mM KCl, 1.36 mM EDTA, 0.5 mM $MgSO_4$, and 0.183 mM PMSF, pH 7.4) following the procedure of Levine et al. [24]. The data are expressed in nmol/mg of protein.

2.10. Catalase and superoxide dismutase activities

Catalase (CAT, EC 1.11.1.6) and superoxide dismutase (Mg^{2+}-SOD, EC 1.15.1.1) activities were performed in diluted aliquots from the supernatants of intestinal homogenates (1:5). CAT activity was assayed in 50 mM potassium phosphate buffer pH 7.4 and 0.3 M H_2O_2 [25]. Mg^{2+}-SOD activity was determined in 1 μM EDTA, 50 mM potassium phosphate buffer, pH 7.8, 13 mM methionine, 75 μM NBT and 40 μM riboflavin [26]. Enzyme activities are expressed in U/mg of protein.

2.11. Nitric oxide levels

The levels of nitric oxide ($NO^{\cdot}$) were determined as total nitrate/nitrite using the Griess reagent [27] with the modification of replacing zinc sulfate by ethanol for protein precipitation in the homogenate supernatant [28]. A standard curve of sodium nitrate was used (1–10 μM). The absorbance was read at 540 nm. The data were expressed as μmol $NO^{\cdot}$/mg of protein.

2.12. IL-6 assay

IL-6 cytokine concentrations in supernatants from intestinal homogenates were quantified by OptEIA ELISA kits (PharMingen Inc., San Diego, CA, USA), according to the manufacturer's instructions. In each assay, 100 μL per well of either recombinant cytokine standards (PharMingen Inc., San Diego, CA, USA) or intestinal supernatants were used. Concentrations were expressed in pg/mg protein.

Table 1
Body weight and serum biochemical parameters.

	Control	FRD	FRD + NAR
Body weight gain (g)	44.33 ± 6.32	80.36 ± 5.37#	60.36 ± 5.95
BMI (kg/m^2)	5.48 ± 0.09	6.58 ± 0.15*	5.52 ± 0.11
Waist circumference (cm)	16.26 ± 0.16	19.10 ± 0.17*	16.68 ± 0.18
Serum Glucose (mg/dL)	136.67 ± 0.07	141.88 ± 0.04	142.25 ± 0.05
Serum Insulin (ng/mL)	1.47 ± 0.08	2.13 ± 0.08*	1.58 ± 0.05
HOMA-IR	5.12 ± 0.32	7.41 ± 0.31*	5.78 ± 0.26
Total cholesterol (mg/dL)	106.66 ± 6.52	105.50 ± 3.94	100.87 ± 5.16
HDL-C (mg/dL)	35.42 ± 2.08	24.33 ± 1.21*	33.75 ± 1.74
LDL-C (mg/dL)	8.18 ± 0.97	8.42 ± 0.41	8.41 ± 0.67
TG (mg/dL)	87.00 ± 8.00	162.50 ± 6.31*	88.25 ± 2.74
TG/HDL-C	2.45 ± 0.17	6.67 ± 0.35*	2.61 ± 0.18
Serum Ca (mg/dL)	9.65 ± 0.11	9.77 ± 0.05	9.83 ± 0.25
Serum P (mg/dL)	5.88 ± 0.18	5.50 ± 0.05	5.50 ± 0.22
25(OH)D_3 (ng/mL)	10.39 ± 0.48	13.37 ± 1.12	13.77 ± 1.32
Serum IL-6 (pg/mL)	19.22 ± 1.59	21.10 ± 7.39	20.12 ± 7.43

Values are expressed as means ± S.E. from 8 rats for each experimental condition; *p < 0.001 *vs* control and FRD + NAR; #p < 0.05 *vs* control and FRD + NAR. FRD: fructose rich diet; NAR: naringin; BMI: body mass index; HOMA-IR: homeostasis model assessment; HDL-C: high density lipoprotein - cholesterol; LDL-C: low density lipoprotein – cholesterol; TG: triglycerides; IL-6: interleukin 6.

2.13. Preparation of nuclear fraction

Nuclear fraction was isolated from intestinal mucosa of each group of animals by differential centrifugation. Intestinal tissue was resuspended in 1 mL of ice-cold buffer A (230 mM Mannitol, 70 mM Sucrose, 1 mM EDTA, 5 mM TrisCl) and homogenized. The homogenate was centrifuged at 1200*g* for 20 min at 4 °C. The supernatant was centrifuged at 2200 × *g* for 20 min at 4 °C, and the pellet was lysed in 1 mL of ice-cold buffer B (230 mM Mannitol, 70 mM Sucrose, 5 mM TrisCl) and was centrifuged at 3000*g* for 20 min at 4 °C. The nuclei then were extracted with 500 μL of ice-cold buffer B and were stored at −80 °C.

2.14. Western blots analysis

Pools of mucosa from two rat duodena were done in RIPA (radio immuno precipitation assay buffer) lysis buffer (1% SDS, 1% Triton X-100, 0.5% sodium deoxycholate in PBS, containing 1 mM PMSF and 1 mM NaF), and then centrifuged. Protein samples (100 μg) were denatured for 5 min at 95 °C and fractionated in 12% (w/v) SDS–polyacrylamide minigels for CB D_{9K}, VDR, CLDN 2, CLDN 12 and nitrotyrosine and in 8% (w/v) SDS–polyacrylamide minigels for the other proteins [29]. Then, they were transferred to nitrocellulose membranes [30]. These membranes (0.45 μm) were blocked for 1.5 h with 2% w/v nonfat dry milk in 0.5 M Tris buffered saline solution and incubated overnight at 4 °C with the specific primary antibody at 1:1000 dilution in each case. The antibodies were: anti-TRPV6 (polyclonal antibody, L-15: sc-31445 Santa Cruz Biotechnology, Santa Cruz, CA, USA), anti-CB_{9K} (monoclonal antibody, Sigma-Aldrich, St. Louis, MO, USA), anti-$PMCA_{1b}$ (human erythrocyte clone 5 F10 A7952 SIGMA Saint Louis, MO, USA), anti-VDR (polyclonal antibody, C-20: sc-1008 Santa Cruz Biotechnology, Santa Cruz, CA, USA), anti-CLDN 2 (monoclonal antibody, Invitrogen, Carlsbad, CA, USA), anti-CLDN 12 (polyclonal antibody, Santa Cruz Biotechnology, Santa Cruz, CA, USA), anti-NFκB p50 (monoclonal antibody, Santa Cruz Biotechnology, Santa

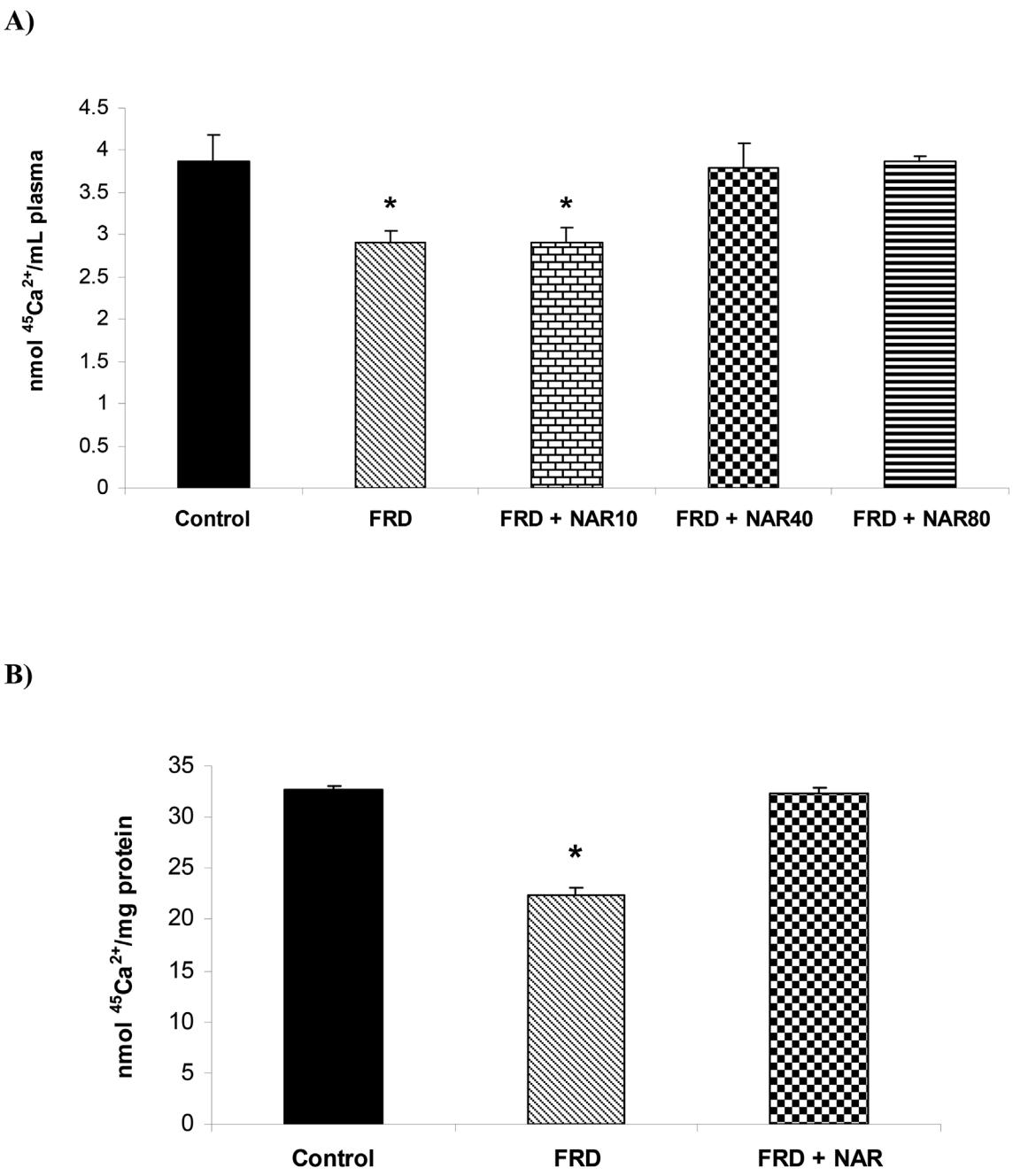

Fig. 2. Effect of FRD, FRD + NAR (10, 40, 80 mg NAR/kg b.w.) or vehicle on intestinal Ca^{2+} absorption in male rats. **A**) One milliliter of 150 mmol/L NaCl, 1 mmol/L $CaCl_2$, containing 1.85×10^5 Bq $^{45}Ca^{2+}$, pH 7.2, was introduced into the lumen of the ligated intestinal segment for 10 min. Then, blood was withdrawn by cardiac puncture, centrifuged and the plasma $^{45}Ca^{2+}$ was measured. **B)** Ca^{2+} uptake by rat enterocytes. Groups: control, FRD and FRD + NAR (40 mg NAR/kg b.w.). Values represent means ± S.E. from 8 rats for each experimental condition. *$p < 0.01$ *vs* control and FRD + NAR.

Cruz, CA, USA), and anti-nitrotyrosine (monoclonal antibody, Santa Cruz Biotechnology, Santa Cruz, CA, USA). After incubation with the primary antibody, membranes were incubated with secondary biotinylated antibodies for 1 h at room temperature. Then, the blots were washed three times and streptavidin - biotin conjugate (Histostain-SP Broad Spectrum, Invitrogen CA, USA) was added. Antigen-antibody complexes were visualized by using 3,3′-diaminobenzidine (DAB) as a chromogen. Monoclonal antibody anti-β-actin (monoclonal antibody, BD Biosciences PharMingen, San Jose, CA, USA), was used to detect β-actin as a marker to normalize the relative expression of the other proteins. The band intensities were quantified using an Image Capturer EC3 Imaging System, Launch VisionWorks LS software (Life Science, Cambridge, UK) in order to obtain the relative expression of proteins.

2.15. Statistics

All results were expressed as means ± S.E. and were analyzed by one way analysis of variance (ANOVA) and the Bonferroni's test as a *post hoc* test. Differences were considered statistically significant at $p < 0.05$. Statistical analysis was performed using SPSS software (version 22.0) for Windows 8.1 (SPSS, Inc., Chicago, IL, USA).

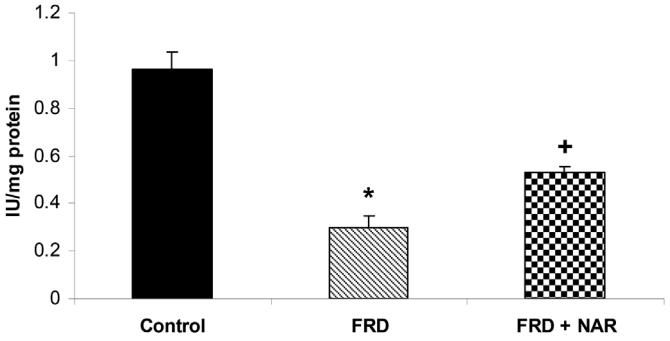

Fig. 3. Intestinal alkaline phophatase activity of duodenal sac from control, FRD and FRD + NAR (40 mg NAR/kg b.w.) rats. Alkaline phosphatase was measured in water homogenates (1:10) of intestinal mucosa using *p*-nitrophenyl phosphate as a substrate in 0.5 M diethanolamine buffer pH 9.8. Values represent means ± S.E. from 6 rats for each experimental condition. *$p < 0.05$ *vs* control and FRD + NAR; $^{+}p < 0.05$ *vs* control.

3. Results

3.1. Morphological parameters and serum profiles of FRD rats treated or not with NAR

Table 1 depicts the morphological parameters and serum profiles of FRD rats treated or not with NAR40 (40 mg/kg b.w.) as compared to control rats. As shown, the body weight gain, the body mass index (BMI) and the waist circumference were higher in FRD rats after 30 days of feeding in comparison with age-matched control rats. NAR40 treatment, injected daily for 4 weeks, blocked all these increments. Serum glucose was similar in the three groups of animals. Serum insulin and the HOMA-IR values were higher in FRD rats than in control animals, effects that were avoided by NAR40 treatment. Total cholesterol remained unchanged as well as the LDL-Cholesterol. However, the levels of HDL-Cholesterol decreased with the FRD, effect that was blocked with NAR. Serum TG was almost double in FRD rats as compared to the control ones, which was avoided by NAR40. Therefore, the TG/HDL-C ratio was much higher in FRD rats, but NAR40 avoided it. Serum calcium, phosphorus, $25(OH)D_3$ and IL-6 were similar among the three groups.

3.2. Intestinal calcium absorption and calcium uptake

FRD rats showed partial inhibition of intestinal Ca^{2+} absorption after 30 days of fructose feeding. NAR10 was unable to avoid this effect, while NAR40 and NAR80 blocked the alteration in the intestinal Ca^{2+} absorption caused by fructose (Fig. 2A). Similarly, Ca^{2+} uptake by mature enterocytes was partially inhibited in FRD rats, which was avoided by NAR40 (Fig. 2B).

3.3. AP activity

The AP activity, an enzyme presumably involved in the intestinal Ca^{2+} absorption, was highly inhibited by the FRD. NAR40 blocked in part this effect, but the AP activity did not reach the control values after 4 weeks of treatment (Fig. 3).

3.4. Protein expression of molecules involved in the transcellular and paracellular pathways of the intestinal Ca^{2+} absorption

Changes in the patterns of protein expression of molecules involved in the transcellular and paracellular pathways of the intestinal Ca^{2+} absorption were quite similar under different conditions. FRD decreased the protein expression of TRPV6, CB D_{9k} and $PMCA_{1b}$, molecules involved in the transcellular pathway, as well as the protein expression of molecules presumably involved in the paracellular pathway such as CLDN 2 and CLDN 12. All these changes were blocked with NAR40 after 4 weeks of administration. VDR protein expression was also decreased by the FRD and NAR40 treatment increased it beyond the control values (Fig. 4).

3.5. Analysis of the intestinal redox state

Table 2 shows the parameters related to the intestinal redox state in FRD rats treated or not with NAR40 as compared to control rats. FRD rats showed half of the intestinal GSH content in comparison with that from the control rats. NAR40 administration increased the intestinal total GSH to almost a double content of that exhibited by the controls. $^{\cdot}O_2^-$ levels were enhanced by the FRD, and the NAR40 treatment went down the values beyond the control ones. Protein carbonyl content was highly enhanced by the FRD, effect that was blocked by NAR40. Both SOD and CAT activities were lower in FRD rats than those from the control rats, but NAR40 administration avoided those responses.

3.6. Nitrergic system

The levels of intestinal $NO^{\cdot}$ were increased by FRD, but NAR40 treatment blocked this effect reaching the $NO^{\cdot}$ levels to values much lower than those from the control rats. Two bands of intestinal proteins mainly exhibited nitration of tyrosine residues. FRD highly increased the nitrosylation of both bands of proteins. NAR 40 treatment avoided the increment in the nitrosylation of band 2 (22 kDa), but not totally that of the band 1 (38 kDa) (Fig. 5).

3.7. Markers of inflammation

Intestinal IL-6 content was increased by FRD, which was blocked by the NAR40 treatment (Fig. 6A). Similarly, the protein expression of nuclear NF-κB from intestinal mucosa was much higher in FRD rats than in control rats; however, NAR40 treatment abolished that effect (Fig. 6B).

4. Discussion

This is the first study showing that NAR, a flavonoid present in grapefruit and other citrus, blocks the inhibition of intestinal Ca^{2+} absorption caused by FRD. The use of these diets in experimental animals is considered as a model of metabolic syndrome. In fact, we have shown that FRD animals have morphological characteristics of this syndrome such as overweight, high BMI and increased waist circumference and some alterations in serum such as low HDL-Cholesterol, enhanced TG and, therefore, an elevated TG/HDL-Cholesterol ratio as well as higher insulin levels and HOMA-IR values. We have proved that all these variables are blocked by daily injection of NAR40 for 4 weeks. It has also been reported that FRD provokes hyperglycemia [31–33], but we did not detect any alteration in serum glucose in FRD rats. This is not surprising since other investigators were not able to show changes in the levels of serum glucose by feeding rats with FRD [9,34]. The reasons for these discrepancies are unclear, but differences in the strain of animals, components of the diet, time of exposure to FRD, levels of insulin could partially explain the different outcomes. NAR changes neither the serum glucose levels nor the serum Ca, P and calcidiol or $25(OH)D_3$, the precursor of $1,25(OH)_2D_3$. Calcidiol is not even altered by FRD. These data are in agreement with those obtained by Douard et al. [35], who have previously found that FRD decreased the serum levels of $1,25(OH)_2D_3$ without perturbing the serum $25(OH)D_3$. The authors suggest that fructose has no effect on the initial step of vitamin D metabolism, but at renal level where either $1,25(OH)_2D_3$ synthesis or degradation occurs. We have also detected no changes in the serum IL-6 produced either by the FRD or the NAR treatment. Merino-Aguilar et al. [36] also did not find alterations in serum IL-6 after feeding rats with FRD. However, NAR has been observed to produce reduction of IL-6 in the liver and primary tumor of rats with Walker 256 carcinosarcoma

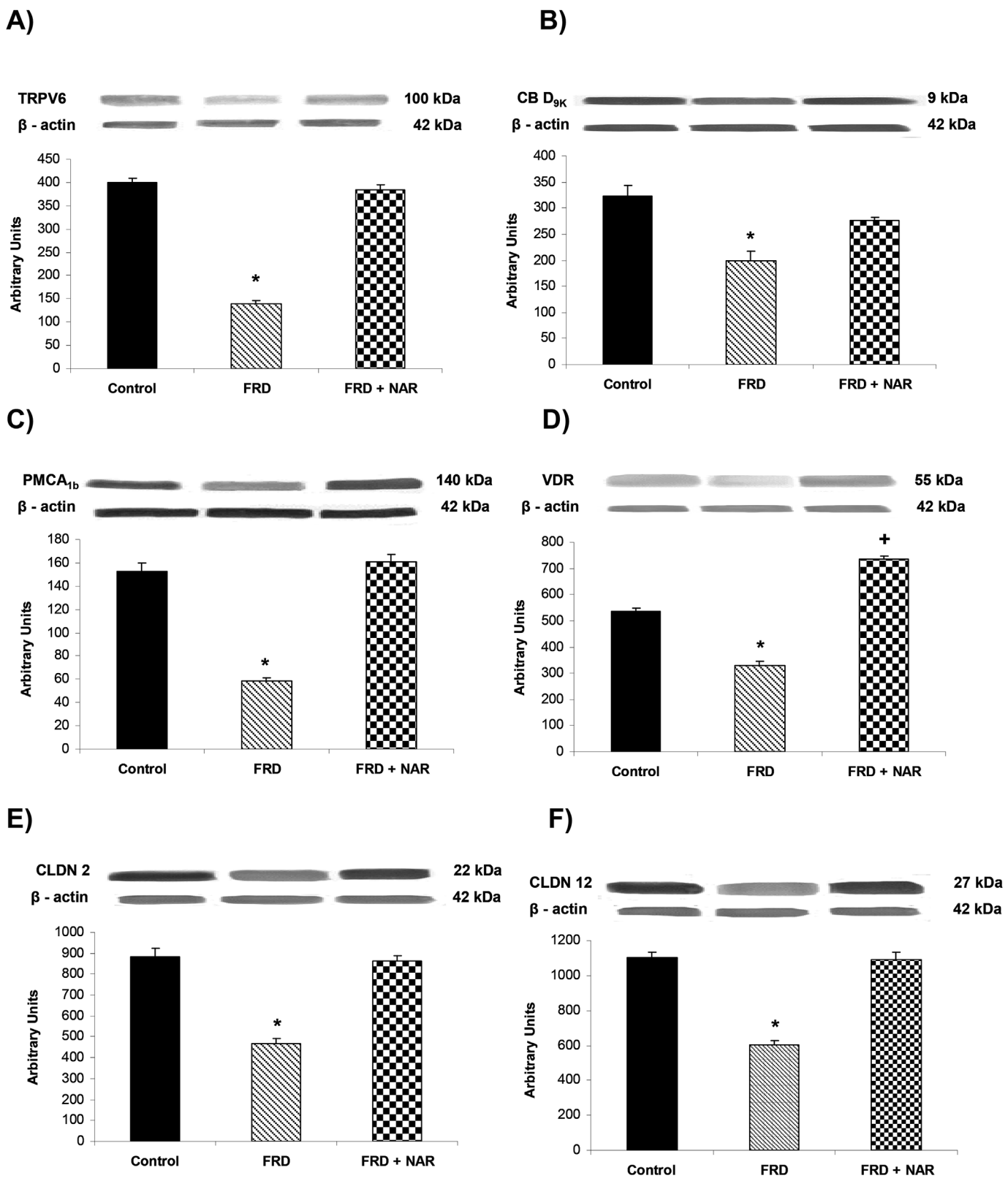

Fig. 4. The protein expression of TRPV6 (**A**), CB_{9K} (**B**), $PMCA_{1b}$ (**C**), VDR (**D**), CLDN 2 (**E**) and CLDN 12 (**F**) was analyzed by Western blot in pool of mucosa from two rat duodenae for each experimental condition: control, FRD and FRD + NAR (40 mg NAR/kg b.w.). Three independent experiments were accomplished. Values are expressed as means ± S.E. *$p < 0.01$ *vs* control and FRD + NAR; $^{+}p < 0.01$ *vs* control.

[37].

As expected, FRD inhibits the intestinal Ca^{2+} absorption and the Ca^{2+} uptake by mature enterocytes. NAR40 avoids those responses normalizing the values to control ones. NAR10 is not able to abrogate the inhibition of intestinal Ca^{2+} absorption caused by FRD and NAR80 produces similar results to those from controls or NAR40. In other words, the protective effect of NAR on intestinal Ca^{2+} absorption is dose dependent to certain extension. Douard et al. [10] have also found

Table 2
Effect of FRD, FRD + NAR or vehicle on total GSH content, superoxide anion content, protein carbonyl, SOD and CAT activities in the rat duodenal mucosa after 30 days of treatment.

Groups	GSH	$^{\cdot}O_2^-$	PROTEIN	SOD	CAT
	(nmol/mg protein)	(NBT reduction, OD)	CARBONYL (nmol/mg protein)	(SOD U/mg protein)	(CAT U/mg protein)
Control	6.33 ± 0.60	0.97 ± 0.05	4.18 ± 0.97	55.93 ± 3.59	12.41 ± 0.67
FRU	2.90 ± 0.99*	1.61 ± 0.12**	15.20 ± 0.96**	38.85 ± 3.77*	7.49 ± 0.37**
FRD + NAR	11.35 ± 1.10$^+$	0.52 ± 0.04$^+$	7.10 ± 0.87	54.73 ± 4.97	11.17 ± 0.43

Values represent means ± S.E. from 8 rats for each experimental condition. *p < 0.05 *vs* control and FRD + NAR; **p < 0.001 *vs* control and FRD + NAR; $^+$p < 0.01 *vs* control. FRD: fructose rich diet; NAR: naringin; GSH: glutathione; $^{\cdot}O_2^-$: superoxide anion; NBT: nitro blue tetrazolium; OD: optical density; SOD: superoxide dismutase; CAT: catalase.

that FRD induced a significant decrease in intestinal Ca^{2+} uptake in male Sprague-Dawley rats. Later on, the same group of investigators [11] have demonstrated that chronic high fructose reduced serum $1,25(OH)_2D_3$ levels in Ca-sufficient rodents, which was always associated with a fructose-induced decrease in CYP27B1 expression, and less consistently with increase in CYP24A, suggesting that fructose might deteriorate the $1,25(OH)_2D_3$ synthesis and enhance the renal catabolism. In addition, they have observed that chronic fructose intake decreases over time normal circulating levels of $1,25(OH)_2D_3$, independently of any increased demand of Ca^{2+}. The $1,25(OH)_2D_3$ depletion could explain, at least in part, the inhibition of intestinal Ca^{2+} absorption since it is the main stimulator of this process. Furthermore, our finding that the intestinal VDR protein expression is diminished by FRD indicates that not only the calciotrope hormone is depleted by the diet, but also its receptor, so it contributes to reducing the intestinal Ca^{2+} absorption. Surprisingly, NAR40 avoids VDR depletion and increases it up beyond the control levels. The reason for this enhancement needs to be further studied.

As known, the intestinal Ca^{2+} absorption occurs through the transcellular and paracellular pathways. FRD alters the protein expression of molecules involved in the transcellular Ca^{2+} transport such as TRPV6, CB D_{9k} and $PMCA_{1b}$ as well as the enzyme activity of AP. TRPV6 is a principal VDR target gene involved in the transcellular pathway of the intestinal calcium absorption. Therefore, the reduction in VDR protein expression caused by FRD could lead to a decrease in the TRPV6 protein expression. CB D_{9k} is a cytoplasmic protein acting not only as a Ca^{2+} ferry from the BBM to the BLM [38], but also as a Ca^{2+} buffer that prevents cell death by apoptosis [39]. As FRD decreases CB D_{9k} expression, the deterioration in the intestinal Ca^{2+} absorption could also be provoked by an increasing in apoptosis of enterocytes. Douard et al. [10] have demonstrated that mRNA expression of CB D_{9k} was also downregulated by the FRD, but they did not find changes in the gene expression of TRPV6, PMCA1 and NCX1. In this study, we have demonstrated that FRD decreases the protein expression of duodenal $PMCA_{1b}$, which might cause a deleterious effect on the Ca^{2+} exit from the enterocytes to the interstitial space. Alzugaray et al. [40] have also demonstrated a decrease in the total PMCA activity in pancreatic islets from FRD rats. Our data indicate that the activity of intestinal AP, another molecule presumably involved in the intestinal Ca^{2+} absorption, is decreased by FRD. In agreement with our data, Felice et al. [41] have detected a decrease in the AP activity in marrow stromal cells isolated from rats with fructose-induced MS. NAR40 is able to block the changes caused by the FRD on the molecules from the transcellular pathway. With regard to CLDN-2 and CLDN-12, proteins located in the intestinal tight junctions and putative molecules from the paracellular Ca^{2+} pathway, it is possible to confirm that both protein expressions are inhibited by FRD, which is blunted by NAR40. Therefore, NAR40 blocks the inhibition of the intestinal Ca^{2+} absorption caused by the FRD *via* protection of the proteins involved either in the transcellular or in the paracellular pathway, perhaps as a consequence of the enhancement of VDR which interacts with its ligand, leading to the normal content of the proteins participating in the intestinal cation transport. Since p38α and GADD45α have been recently reported to be involved in the enhancement of TRPV6 expression by vitamin D [42], the participation of those molecules in the TRPV6 response to NAR treatment is a possibility that needs to be investigated. In addition, the capacity of NAR to increase ATP levels as shown in pancreatic β cells [43] could also contribute to the normalization of the intestinal Ca^{2+} absorption, since it is an ATP-dependent process [44].

We have previously demonstrated that the maintenance of the steady state levels of intestinal GSH is essential to obtain an optimal Ca^{2+} absorption [2,3]. The decrease in the GSH content in the intestine from FRD rats indicates that the exacerbation of dietary fructose alters the intestinal redox state leading to oxidative stress. The increments in the $^{\cdot}O_2^-$ and in the carbonyl contents as well as the decreases in SOD and CAT activities, enzymes of the antioxidant defense, result in impairment of the redox equilibrium, which contributes to altering in the intestinal Ca^{2+} absorption. Kanappam et al. [8] have also demonstrated that FRD decrease the GSH content and the antioxidant enzyme activities as well as vitamin C and vitamin E levels in the liver and skeletal muscle from rats. NAR40 is able to block all the alterations in the redox system, which means that NAR protects the intestinal Ca^{2+} absorption through its antioxidant properties. It is largely known that NAR has antioxidant actions under oxidant conditions [45–47].

Another mechanism involved in the inhibition of intestinal Ca^{2+} absorption caused by FRD is the alteration of the nitrergic system. In fact, FRD increases the $NO^{\cdot}$ content and the nitrotyrosine content of proteins of 22 and 38 kDa from rat intestine. NAR not only avoids the increase in the levels of NO, but also decreases them to values much lower than the control ones. NAR 40 treatment blocks the increment in the nitrosylation of 38 kDa band, but not totally that of the 22 kDa band. By contrast, FRD has shown to decrease the levels of nitrite in the plasma, liver and skeletal muscle, effects that were abolished by NAR [8]. He et al. [48] have demonstrated increased expression of inducible $NO^{\cdot}$ synthase by high fructose diet. This might occur in the rat intestine, which would explain the augmentation in the $NO^{\cdot}$ levels by FRD. $NO^{\cdot}$ would interact with superoxide anions forming the highly toxic peroxynitrite ($ONOO^{\cdot}$), which nitrosylates thiol, hydroxyl and amine groups of biological molecules. In fact, our data show that FRD increases nitrosylation of intestinal proteins and Kanappam et al. [8] have demonstrated increases in nitrosothiols in the plasma, liver and skeletal muscle. Therefore, altogether indicates that nitrosative stress occurs after chronic fructose intake. The attenuation of the oxidative and nitrosative stress by NAR could be due to the phenolic groups and a keto group which can react with hydroxyl radicals, hydrogen peroxide and peroxynitrite.

Although at systemic level IL-6 remains unchanged in FRD rats with or without NAR treatment, in the intestine the IL-6 content and the protein expression of NF-κB are increased by FRD, effects that are abolished by chronic NAR treatment. NF-κB is a transcription factor involved in important physiological process, among them in the control of genes activated upon inflammation [49]. IL-6 is an inflammatory cytokine, whose gene has in its promotor region a site that binds NFkB. The increase in both IL-6 and NF-κB by FRD is indicative that the inflammation is involved in the inhibitory effect of chronic fructose on the intestinal Ca^{2+} absorption. The link between the FRD and the

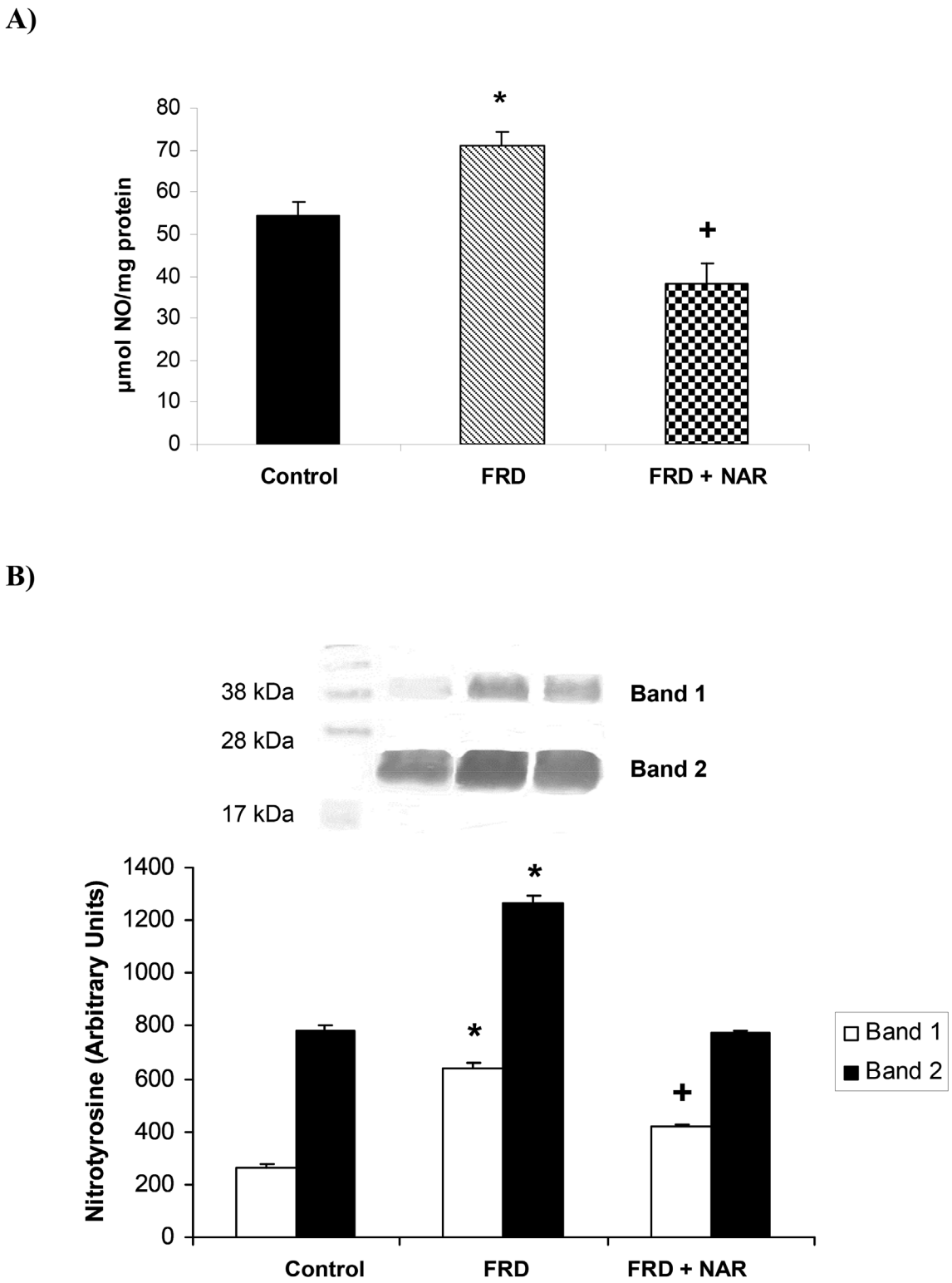

Fig. 5. Effect of FRD, FRD + NAR (40 mg NAR/kg b.w.) or vehicle on: **A)** NO level measured by Griess assay in the duodenal mucosa from 6 rats for each experimental condition. Values are expressed as means ± S.E. *p < 0.01 *vs* control and FRD + NAR; $^{+}$p < 0.05 *vs* control; **B)** nitrotyrosine expression was analyzed by Western blot in pool of mucosa from two rat duodenae for each experimental condition. Three independent experiments were accomplished. Values are expressed as means ± S.E. *p < 0.01 *vs* Band 1 or Band 2 from control, respectively, and Band 1 or Band 2 from FRD + NAR, respectively; $^{+}$p < 0.05 *vs* Band 1 from control.

inflammation has been largely described [50–52]. There is also evidence that NAR has anti-inflammatory effects [53–55].

To conclude, FRD inhibits the intestinal Ca^{2+} absorption by decreasing the protein expression of TRPV6, CB D_{9k} and $PMCA_{1b}$, molecules of the transcellular Ca^{2+} pathway, and those from the Cldn-2 and Cldn-12, proteins of the tight junctions, presumably involved in the paracellular pathway. The depletion in VDR levels caused by high fructose, in addition to the low levels of $1,25(OH)_2D_3$, could be responsible for the low content of those Ca^{2+} transporters. Besides, the oxidative and nitrosative stress and the inflammation would contribute

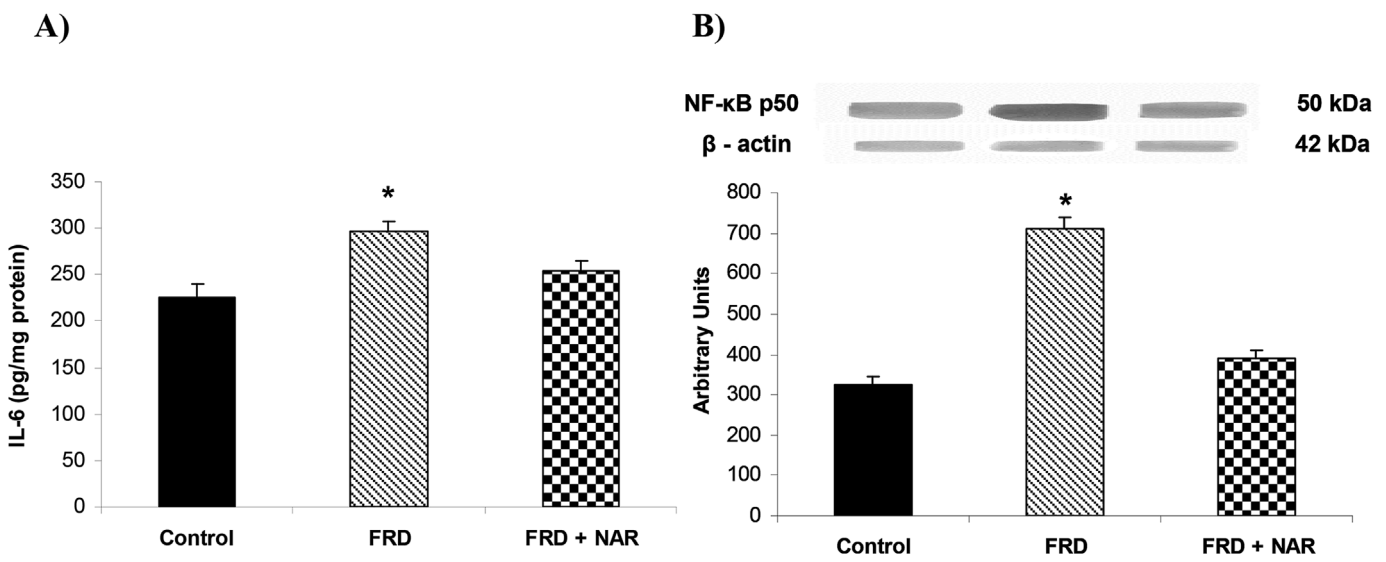

Fig. 6. Effect of FRD, FRD + NAR (40 mg NAR/kg b.w.) or vehicle on: **A)** IL-6 in the supernatants from rat duodenal mucosa was assayed by quantitative ELISA. Four rats were used for each experimental condition. All assays were performed in duplicate; **B)** protein expression of NF-κB p50 in nuclear extract from rat enterocytes. Values are expressed as means ± S.E. *p < 0.05 *vs* control and FRD + NAR.

to reducing the capability of those molecules to transport Ca^{2+}. NAR is able to abolish all the responses by triggering its anti-oxidant, anti-nitrergic and anti-inflammatory properties. The data indicate that NAR is a potential therapeutic agent to normalize the intestinal Ca^{2+} absorption in conditions of chronic high fructose intake.

Acknowledgements

This work was supported by Grants from FonCyT (PICT 2015-386), Ministerio de Ciencia de la Provincia de Córdoba (GRFT-2015), CONICET (PIP 2013–2015) and SECYT (UNC 2016-2017), Argentina. Special thanks from the authors to GEPSA (Grupo Pilar S.A.) and the Fundación de la Facultad de Ciencias Médicas for donation of the animal feeding. Prof. Dr. Nori Tolosa de Talamoni and Dr. Valeria Rodríguez are Members of Investigator Career from the Consejo Nacional de Investigaciones Científicas y Tecnológicas (CONICET). Solangue Guizzardi is the recipient of a CONICET fellowship. All of the authors participated in the conception, design, and performance of the study as well as interpretation of data and drafting the manuscript. None of the authors had a personal conflict of interest associated with this work.

References

[1] G. Diaz de Barboza, S. Guizzardi, L. Moine, N. Tolosa de Talamoni, Oxidative stress, antioxidants and intestinal calcium absorption, World J. Gastroenterol. 23 (2017) 2841–2853.
[2] N. Tolosa de Talamoni, A. Marchionatti, V. Baudino, A. Alisio, Glutathione plays a role in the chick intestinal calcium absorption, Comp. Biochem. Physiol. A Physiol. 115 (1996) 127–132.
[3] A.M. Marchionatti, G.E. Díaz de Barboza, V.A. Centeno, A.E. Alisio, N.G. Tolosa de Talamoni, Effects of a single dose of menadione on the intestinal calcium absorption and associated variables, J. Nutr. Biochem. 14 (2003) 466–472.
[4] A.M. Marchionatti, A.V. Perez, G.E. Diaz de Barboza, B.M. Pereira, N.G. Tolosa de Talamoni, Mitochondrial dysfunction is responsible for the intestinal calcium absorption inhibition induced by menadione, Biochim. Biophys. Acta 1780 (2008) 101–107.
[5] T.E. Woudenberg-Vrenken, A.L. Lameris, P. Weißgerber, J. Olausson, V. Flockerzi, R.J. Bindels, M. Freichel, J.G. Hoenderop, Functional TRPV6 channels are crucial for transepithelial Ca2+ absorption, Am. J. Physiol. Gastrointest. Liver Physiol. 303 (2012) G879–G885.
[6] G. Diaz de Barboza, S. Guizzardi, N. Tolosa de Talamoni, Molecular aspects of intestinal calcium absorption, World J. Gastroenterol. 21 (2015) 7142–7154.
[7] H. Fujita, K. Sugimoto, S. Inatomi, T. Maeda, M. Osanai, Y. Uchiyama, Y. Yamamoto, T. Wada, T. Kojima, H. Yokozaki, T. Yamashita, S. Kato, N. Sawada, H. Chiba, Tight junction proteins claudin-2 and -12 are critical for vitamin D-dependent Ca2+ absorption between enterocytes, Mol. Biol. Cell 19 (2008) 1912–1921.
[8] S. Kannappan, N. Palanisamy, C.V. Anuradha, Suppression of hepatic oxidative events and regulation of eNOS expression in the liver by naringenin in fructose-administered rats, Eur. J. Pharmacol. 645 (2010) 177–184.
[9] A.S. Londero, M.R. Arana, V.G. Perdomo, G.N. Tocchetti, F. Zecchinati, C.I. Ghanem, M.L. Ruiz, J.P. Rigalli, A.D. Mottino, F. García, S.S. Villanueva, Intestinal multidrug resistance-associated protein 2 is down-regulated in fructose-fed rats, J. Nutr. Biochem. 40 (2017) 178–186.
[10] V. Douard, A. Asgerally, Y. Sabbagh, S. Sugiura, S.A. Shapses, D. Casirola, R.P. Ferraris, Dietary fructose inhibits intestinal calcium absorption and induces vitamin D insufficiency in CKD, J. Am. Soc. Nephrol. 2 (2010) 261–271.
[11] V. Douard, C. Patel, J. Lee, P. Tharabenjasin, E. Williams, J.C. Fritton, Y. Sabbagh, R.P. Ferraris, Chronic high fructose intake reduces serum 1,25 (OH)2D3 levels in calcium-sufficient rodents, PLoS One 9 (2014) e93611.
[12] L. Cigliano, M.S. Spagnuolo, R. Crescenzo, R. Cancelliere, L. Iannotta, A. Mazzoli, G. Liverini, S. Iossa, Short-term fructose feeding induces inflammation and oxidative stress in the hippocampus of young and adult rats, Mol. Neurobiol. (2017), https://doi.org/10.1007/s12035-017-0518-2.
[13] A. Rosas-Villegas, M. Sánchez-Tapia, A. Avila-Nava, V. Ramírez, A.R. Tovar, N. Torres, Differential effect of sucrose and fructose in combination with a high fat diet on intestinal microbiota and kidney oxidative stress, Nutrients (2017), https://doi.org/10.3390/nu9040393.
[14] W.C. Dornas, L.M. Cardoso, M. Silva, N.L. Machado, D.A. Chianca Jr., A.C. Alzamora, W.G. Lima, V. Lagente, M.E. Silva, Oxidative stress causes hypertension and activation of nuclear factor-κB after high-fructose and salt treatments, Sci. Rep. 7 (2017) 46051.
[15] C. Faggio, A. Sureda, S. Morabito, A. Sanches-Silva, A. Mocan, S.F. Nabavi, S.M. Nabavi, Flavonoids and platelet aggregation: a brief review, Eur. J. Pharmacol. 807 (2017) 91–101.
[16] Z. Qi, Y. Xu, Z. Liang, S. Li, J. Wang, Y. Wei, B. Dong, Naringin ameliorates cognitive deficits via oxidative stress, proinflammatory factors and the PPARγ signaling pathway in a type 2 diabetic rat model, Mol. Med. Rep. 12 (2015) 7093–7101.
[17] R. Chen, Q.L. Qi, M.T. Wang, Q.Y. Li, Therapeutic potential of naringin: an overview, Pharm. Biol. 54 (2016) 3203–3210.
[18] M.A. Alam, N. Subhan, M.M. Rahman, S.J. Uddin, H.M. Reza, S.D. Sarker, Effect of citrus flavonoids, naringin and naringenin, on metabolic syndrome and their mechanisms of action, Adv. Nutr. 5 (2014) 404–417.
[19] D.R. Matthews, J.P. Hosker, A.S. Rudenski, B.A. Naylor, D.F. Treacher, R.C. Turner, Homeostasis model assessment: insulin resistance and beta-cell function from fasting plasma glucose and insulin concentrations in man, Diabetologia 28 (1985) 412–419.
[20] V. Centeno, G. Díaz de Barboza, A. Marchionatti, M. Alisio, R. Dallorso, N. Nasif, N. Tolosa de Talamoni, Dietary calcium deficiency increases Ca2+ uptake and Ca2+ extrusion mechanisms in chick enterocytes, Comp. Biochem. Physiol. A Mol. Integr. Physiol. 139 (2004) 133–141.
[21] C.T. Liang, J. Barnes, B. Sacktor, S. Takamoto, Alterations of duodenal vitamin D-dependent calcium-binding protein content and calcium uptake in brush border membrane vesicles in aged Wistar rats: role of 1,25-dihydroxyvitamin D3, Endocrinology 128 (1991) 1780–1784.
[22] M.E. Anderson, Determination of glutathione and glutathione disulfide in biological samples, Methods Enzymol. 113 (1985) 548–555.
[23] L. Serrander, L. Cartier, K. Bedard, B. Banfi, B. Lardy, O. Plastre, A. Sienkiewicz, L. Fórró, W. Schlegel, K.H. Krause, NOX4 activity is determined by mRNA levels and reveals a unique pattern of ROS generation, Biochem. J. 406 (2007) 105–114.
[24] R.L. Levine, D. Garland, C.N. Oliver, A. Amici, I. Climent, A.G. Lenz, B.W. Ahn,

S. Shaltiel, E.R. Stadtman, Determination of carbonyl content in oxidatively modified proteins, Methods Enzymol. 186 (1990) 464–478.
[25] H. Aebi, S.R. Wyss, B. Scherz, F. Skvaril, Heterogeneity of erythrocyte catalase II. Isolation and characterization of normal and variant erythrocyte catalase and their subunits, Eur. J. Biochem. 48 (1974) 137–145.
[26] C.O. Beauchamp, I. Fridovich, Isozymes of superoxide dismutase from wheat germ, Biochim. Biophys. Acta 317 (1973) 50–64.
[27] K.M. Miranda, M.G. Espey, D.A. Wink, A rapid, simple spectrophotometric method for simultaneous detection of nitrate and nitrite, Nitric Oxide 5 (2001) 62–71.
[28] H.H. Arab, S.A. Salama, A.H. Eid, H.A. Omar, S.A. Arafa, I.A Maghrabi, Camel's milk ameliorates TNBS-induced colitis in rats via downregulation of inflammatory cytokines and oxidative stress, Food Chem. Toxicol. 69 (2014) 294–302.
[29] U.K. Laemmli, Cleavage of structural proteins during the assembly of the head of bacteriophage T4, Nature 227 (1970) 680–685.
[30] H. Towbin, T. Staehelin, J. Gordon, Electrophoretic transfer of proteins from polyacrylamide gels to nitrocellulose sheets: procedure and some applications, Biotechnology 24 (1992) 145–149.
[31] S.R. Blakely, J. Hallfrisch, S. Reiser, E.S. Prather, Long-term effects of moderate fructose feeding on glucose tolerance parameters in rats, J. Nutr. 111 (1981) 307–314.
[32] L. Tappy, K.A. Lê, Metabolic effects of fructose and the worldwide increase in obesity, Physiol. Rev. 90 (2010) 23–46.
[33] J.A. Moreno, E. Hong, A single oral dose of fructose induces some features of metabolic syndrome in rats: role of oxidative stress, Nutr. Metab. Cardiovasc. Dis. 23 (2013) 536–542.
[34] S. Yoo, H. Ahn, Y.K. Park, High dietary fructose intake on cardiovascular disease related parameters in growing rats, Nutrients (2016), https://doi.org/10.3390/nu9010011.
[35] V. Douard, T. Suzuki, Y. Sabbagh, J. Lee, S. Shapses, S. Lin, R.P. Ferraris, Dietary fructose inhibits lactation-induced adaptations in rat 1,25-$(OH)_2D_3$ synthesis and calcium transport, FASEB J. 26 (2012) 707–721.
[36] H. Merino-Aguilar, D. Arrieta-Baez, M. Jiménez-Estrada, G. Magos-Guerrero, R.J. Hernández-Bautista, C. Susunaga-Notario Adel, J.C. Almanza-Pérez, G. Blancas-Flores, R. Román-Ramos, F.J. Alarcón-Aguilar, Effect of fructooligosaccharides fraction from Psacalium decompositum on inflammation and dyslipidemia in rats with fructose-induced obesity, Nutrients 6 (2014) 591–604.
[37] C.A. Camargo, M.C. Gomes-Marcondes, N.C. Wutzki, H. Aoyama, Naringin inhibits tumor growth and reduces interleukin-6 and tumor necrosis factor α levels in rats with Walker 256 carcinosarcoma, Anticancer Res. 32 (2012) 129–133.
[38] N. Tolosa de Talamoni, A. Perez, A. Alisio, Effect of cholecalciferol on intestinal epithelial cells, Trends Comp. Biochem. Physiol 5 (1998) 179–185.
[39] S. Christakos, Y. Liu, Biological actions and mechanism of action of calbindin in the process of apoptosis, J. Steroid Biochem. Mol. Biol. 89–90 (2004) 401–404.
[40] M.E. Alzugaray, M.E. García, H.H. Del Zotto, M.A. Raschia, J. Palomeque, J.P. Rossi, J.J. Gagliardino, L.E. Flores, Changes in islet plasma membrane calcium-ATPase activity and isoform expression induced by insulin resistance, Arch. Biochem. Biophys. 490 (2009) 17–23.
[41] J.I. Felice, M.V. Gangoiti, M.S. Molinuevo, A.D. McCarthy, A.M. Cortizo, Effects of a metabolic syndrome induced by a fructose-rich diet on bone metabolism in rats, Metabolism 63 (2014) 296–305.
[42] M. Ishizawa, D. Akagi, J. Yamamoto, M. Makishima, 1α,25-Dihydroxyvitamin D3 enhances TRPV6 transcription through p38 MAPK activation and GADD45 expression, J. Steroid Biochem. Mol. Biol. 172 (2017) 55–61.
[43] S. Nzuza, D.E. Ndwandwe, P.M. Owira, Naringin protects against HIV-1 protease inhibitors-induced pancreatic β-cell dysfunction and apoptosis, Mol. Cell Endocrinol. 437 (2016) 1–10.
[44] R.H. Wasserman, Comments on the essentiality of calbindin-D9k and calcium channel TRPV6 for optimal active intestinal calcium transport in vitro, Ann. N. Y. Acad. Sci. 1192 (2010) 365–366.
[45] A. Visnagri, M. Adil, A.D. Kandhare, S.L. Bodhankar, Effect of naringin on hemodynamic changes and left ventricular function in renal artery occluded renovascular hypertension in rats, J. Pharm. Bioallied Sci. 7 (2015) 121–127.
[46] N. Wang, F. Zhang, L. Yang, J. Zou, H. Wang, K. Liu, M. Liu, H. Zhang, X. Xiao, K. Wang, Resveratrol protects against L-arginine-induced acute necrotizing pancreatitis in mice by enhancing SIRT1-mediated deacetylation of p53 and heat shock factor 1, Int. J. Mol. Med. (2017), https://doi.org/10.3892/ijmm.2017.3012.
[47] M. Jamalan, M.A. Ghaffari, P. Hoseinzadeh, M. Hashemitabar, M. Zeinali, Human sperm quality and metal toxicants: protective effects of some flavonoids on male reproductive function, Int. J. Fertil. Steril. 10 (2016) 215–223.
[48] S. He, H. Rehman, G.L. Wright, Z. Zhong, Inhibition of inducible nitric oxide synthase prevents mitochondrial damage and improves survival of steatotic partial liver grafts, Transplantation 89 (2010) 291–298.
[49] T.A. Libermann, D. Baltimore, Activation of interleukin-6 gene expression through the NF-kappa B transcription factor, Mol. Cell Biol. 10 (1990) 2327–2334.
[50] S. Incir, I.M. Bolayirli, O. Inan, M.S. Aydın, I.A. Bilgin, I. Sayan, M. Esrefoglu, A. Seven, The effects of genistein supplementation on fructose induced insulin resistance, oxidative stress and inflammation, Life Sci. 158 (2016) 57–62.
[51] P.D. Prince, C.R. Lanzi, J.E. Toblli, R. Elesgaray, P.I. Oteiza, C.G. Fraga, M. Galleano, Dietary (-)-epicatechin mitigates oxidative stress, NO metabolism alterations, and inflammation in renal cortex from fructose-fed rats, Free Radic. Biol. Med. 90 (2016) 35–46.
[52] D.F. Rodrigues, M.C. Henriques, M.C. Oliveira, Z. Menezes-Garcia, P.E. Marques, G. Souza Dda, G.B. Menezes, M.M. Teixeira, A.V. Ferreira, Acute intake of a high-fructose diet alters the balance of adipokine concentrations and induces neutrophil influx in the liver, J. Nutr. Biochem. 25 (2014) 388–394.
[53] T.A. Zimmers, M.L. Fishel, A. Bonetto, STAT3 in the systemic inflammation of cancer cachexia, Semin. Cell Dev. Biol. 54 (2016) 28–41.
[54] K. Liu, L. Wu, X. Shi, F. Wu, Protective effect of naringin against ankylosing spondylitis via ossification, inflammation and oxidative stress in mice, Exp. Ther. Med. 12 (2016) 1153–1158.
[55] M. Gil, Y.K. Kim, S.B. Hong, K.J. Lee, Naringin decreases TNF-α and HMGB1 release from LPS-stimulated macrophages and improves survival in a CLP-induced sepsis mice, PLoS One 11 (2016) e0164186.